Macroscopic resonant tunneling of magnetic flux

D. V. Averin, Jonathan R. Friedman, and J. E. Lukens
Department of Physics and Astronomy, SUNY at Stony Brook, Stony Brook, New York 11794
(Received 3 May 2000)

We have developed a quantitative theory of resonant tunneling of magnetic flux between discrete macroscopically distinct quantum states in superconducting quantum interference device systems. The theory is based on the standard density-matrix approach. Its elements include the discussion of the two different relaxation mechanisms that exist for the double-well potential, and description of the ''photon-assisted'' tunneling driven by external rf radiation. It is shown that in the case of coherent flux dynamics, rf radiation should lead to splitting of the peaks of resonant flux tunneling, indicating that the resonant tunneling is a convenient tool for studying macroscopic quantum coherence of flux.

I. INTRODUCTION

Bose condensates of Cooper pairs in superconductors have a remakable ability to populate a single quantum state with a macroscopically large number of particles. This property of the Cooper pair condensates leads to macroscopic quantum effects in the dynamics of Josephson junctions, i.e., makes it possible for a Josephson junction to behave largely as a pure quantum state of a simple quantum mechanical system while still containing macroscopically large number of Cooper pairs. Due to the strongly nonlinear character of the Josephson dynamics even in the classical regime, macroscopic quantum effects can be quite nontrivial. They have been known for the past twenty years—see reviews in Ref. 1, and are continuing to attract considerable interest.[2] This interest is to a large extent stimulated by the challenge to our understanding of the foundations of the quantum theory presented by direct manifestations of quantum mechanics at the macroscopic level.[3–5] Another recent motivation for studying quantum effect in Josephson dynamics is provided by possible applications to quantum computation.[6–9]

The most advanced macroscopic quantum effect observed experimentally up to now is resonant tunneling between quantized energy levels in the adjacent wells of the Josephson potential.[10,11] The aim of this work is to develop a theory of this phenomenon in superconducting quantum interference device (SQUID) systems, where the potential contains two wells, each with a different value of the average magnetic flux. We consider the regime of weak energy dissipation important for studying coherent effects in resonant tunneling. This regime has not been discussed appropriately in the existing treatments of resonant tunneling in double-well potentials[12–14] or multiwell potentials corresponding to the current-biased Josephson junctions.[15,16] The most essential new feature of our approach is an account of the two types of relaxation mechanisms, intrawell and interwell, that exist in the system. The two relaxation mechanisms are very different in their dependence on the parameters of the SQUID potential, and lead to different shapes of the resonant tunneling peaks. Differences in relaxation mechanisms also make macroscopic resonant tunneling of flux different from the otherwise very similar ''mesoscopic'' resonant tunneling between charge states of small Josephson junctions[17,18] and electron states in quantum dots.[19–21]

Another new element of this work is the discussion of the ''photon-assisted'' macroscopic resonant flux tunneling under rf irradiation. We show that in contrast to tunneling under stationary-bias conditions, the peaks of the photon-assisted tunneling depend qualitatively on the strength of decoherence in the flux dynamics. In the case of coherent flux dynamics, the resonant peaks of the photon-assisted tunneling are split in two. The splitting reflects the coherent hybridization of the macroscopic flux states in the two wells of the SQUID potential and is suppressed with increasing rate of decoherence. Very recently, such a splitting of the resonant flux-tunneling peaks has been observed experimentally,[22] demonstrating the quantum coherence of the macroscopically distinct flux states.[22,23] The paper is organized as follows. In Sec. II we derive the evolution equations for the density matrix describing the resonant flux tunneling under stationary-bias conditions, and introduce the two relaxation mechanisms for tunneling dynamics. Using these equations, we calculate the rate of flux tunneling in Sec. III. In Sec. IV, we extend the results of Secs. II and III to the case of photon-assisted tunneling.

II. EQUATIONS FOR THE DENSITY MATRIX

To derive equations for the density matrix in the regime of resonant tunneling of magnetic flux Φ we consider the standard model of the phase dynamics in SQUID's. The combination of the magnetic energy of the SQUID loop biased with an external flux and the Josephson coupling energy of the SQUID junctions (for details, see, e.g., Ref. 24) produces the double-well potential $U(\Phi)$ for Φ evolution (shown schematically in Fig. 1 below). The main part of the Hamiltonian governing the flux dynamics consists of the potential $U(\Phi)$ and the charging energy of the junction capacitance C:

$$H_0=\frac{Q^2}{2C}+U(\Phi). \tag{1}$$

The charge Q on the junction capacitance and the flux Φ satisfy standard commutation relations $[\Phi,Q]=i\hbar$.

The two wells of the potential $U(\Phi)$ have discrete energy states ε_{jn} with characteristic energy separation on the order of ω_j, where $j=1,2$ is the well index, ω_j are the oscillation

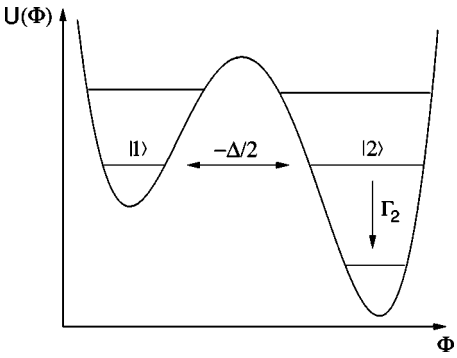

FIG. 1. Schematic diagram of the macroscopic resonant tunneling of flux Φ in the double-well potential $U(\Phi)$ at low temperatures under stationary-bias conditions. The flux tunnels out of ground state $|1\rangle$ in the left well coupled with the amplitude $-\Delta/2$ to the resonant state $|2\rangle$ in the right well, where it decays with the rate Γ_2 into the lower states in this well.

frequencies around the potential minima, and $n=0,1,\ldots,$ numbers the states within each well. The two frequencies ω_j have the same order of magnitude $\omega_1 \sim \omega_2 \equiv \omega_p$. External magnetic flux controls the energy difference between the states in opposite wells. Away from the resonance conditions, when all the energies ε_{jn} are separated by large energy gaps of order ω_p, the states $|jn\rangle$ are localized within the jth well, and the amplitude of the wave functions $\psi_{jn}(\Phi)$ in the opposite well is very small. However, when the energies of the two states $|1\rangle \equiv |1n_1\rangle$ and $|2\rangle \equiv |2n_2\rangle$ are close, $|\varepsilon| \ll \omega_p$, where $\varepsilon \equiv \varepsilon_{1n_1} - \varepsilon_{2n_2}$, these states become strongly coupled, and the wave functions spread over the both wells. As shown in the Appendix, strong coupling of the states $|1,2\rangle$ at resonance can be described by the tunneling amplitude Δ, and the Hamiltonian (1) reduces to the regular two-state form in the basis of these states:

$$H_0 = \frac{1}{2}[\varepsilon(|1\rangle\langle 1| - |2\rangle\langle 2|) - \Delta(|1\rangle\langle 2| + |2\rangle\langle 1|)], \quad (2)$$

$$\Delta = (\omega_1 \omega_2)^{1/2} D/\pi,$$

where D is the quantum mechanical transparency of the barrier separating the wells.

Without perturbations, the two-state dynamics described by Eq. (2) is decoupled from the other states of the Hamiltonian (1). The most important perturbation creating such coupling is the energy dissipation that induces transitions between the states $|1,2\rangle$ and other states $|jn\rangle$. In the relevant temperature range below superconducting energy gap of the junction electrodes, the quasiparticle tunneling is suppressed and the main source of energy dissipation is the electromagnetic environment of the system. Under the assumption that the electromagnetic modes of the environment are in equilibrium at temperature T, and are well described by linear electrodynamics, the interaction between the flux Φ and the heat bath of these modes can be written as

$$V = -I_f \Phi. \quad (3)$$

Here I_f is the fluctuating current created in the SQUID loop by the environment, with the correlation function given by the fluctuation-dissipation theorem:

$$\langle I_f(t) I_f(t+\tau)\rangle = \int \frac{d\omega}{\pi} \frac{\omega G(\omega) e^{i\omega\tau}}{1 - e^{-\omega/T}}, \quad (4)$$

where the angle brackets denote averaging over the equilibrium density matrix of the environment, and $G(\omega)$ is the dissipative part of the environment conductance. Equation (4) is sufficient to characterize completely the effects of the weak energy dissipation considered in this work. For arbitrary dissipation strength, one can use the Caldeira-Leggett model[25] to express explicitly the environment Hamiltonian and the current operator I_f in terms of a set of harmonic oscillators.

The interaction (3) induces both ''vertical'' transitions within each well and direct interwell transitions. In terms of the two-state dynamics with the Hamiltonian (2), the latter correspond to the modulation of the tunneling amplitude Δ by the environment. The matrix elements of this type of interwell transitions are, however, smaller by a factor of Δ/ω_p than those of the intrawell transitions. The small matrix elements can be neglected under the conditions of resonance, when the flux tunneling between the two wells is dominated by the stronger resonant processes. In this approximation, we can omit the terms in the flux operator in the interaction (3) that are nondiagonal in the well index j:

$$\Phi = \sum_{j,n,n'} \Phi^{(j)}_{n,n'} |jn\rangle\langle jn'|. \quad (5)$$

Here $\Phi^{(j)}_{n,n'}$ are the matrix elements of Φ in the $|jn\rangle$ basis. The perturbation (3) with the flux operator (5) has two effects on the dynamics of the states $|1,2\rangle$. The first is fluctuations of the energy difference ε, which induce transitions between these states and lead to the loss of mutual coherence between them. The part of the Φ operator (5) responsible for these fluctuations can be written as $\delta\Phi(|1\rangle\langle 1| - |2\rangle\langle 2|)$, where $\delta\Phi$ is half of the difference between the average flux values in the states $|1\rangle$ and $|2\rangle$. The remaining terms in Eq. (5) induce intrawell transitions from the states $|1\rangle$ and $|2\rangle$ to the other states in the corresponding wells.

For weak dissipation both effects can be described quantitatively by the standard density matrix technique—see, e.g., Ref. 26. The description starts from the equation for the evolution of the density matrix ρ, obtained treating the coupling V (3) in second-order perturbation theory:

$$\dot{\rho}(t) = -i[H_0, \rho] - \int^t d\tau \langle [V(t), [V(\tau), \rho(\tau)]]\rangle. \quad (6)$$

If the environment has a large cutoff frequency $\omega_c \gg \varepsilon, \Delta$, the density matrix evolves slowly on the time scale of variations of $V(t)$, and we can make the Markov approximation $\rho(\tau) \simeq \rho(t)$ in the last term of Eq. (6). The condition of weak dissipation also allows us to keep only the dissipative terms in Eq. (6) that do not oscillate in time with frequencies of the main Hamiltonian H_0, since only these terms lead to effects that accumulate with time. Using these approximations to evaluate the dissipative part of the Eq. (6), we obtain the final equation for the density matrix in the basis of resonant states $|1,2\rangle$ relevant for the transfer of flux between the wells:

$$\dot{\rho} = -i[H_0, \rho] + \Gamma[\rho] + \gamma[\rho]. \tag{7}$$

The term Γ in this equation describes the effect of the intrawell transitions from the states $|1\rangle$ and $|2\rangle$:

$$\Gamma[\rho] = -\begin{pmatrix} \Gamma_1\rho_{11}, & (\Gamma_1+\Gamma_2)\rho_{12}/2 \\ (\Gamma_1+\Gamma_2)\rho_{21}/2, & \Gamma_2\rho_{22} \end{pmatrix}. \tag{8}$$

At temperatures smaller than energy separation in the wells, the total decay rate Γ_j in Eq. (8) of the state $|j\rangle$ into the states with lower energy in the same well is

$$\Gamma_j = \sum_{n<n_j} \frac{2|\Phi^{(j)}_{n,n_j}|^2}{\hbar^2}(\varepsilon_{n_j}-\varepsilon_n)G(\varepsilon_{n_j}-\varepsilon_n).$$

The second dissipation term $\gamma[\rho]$ in Eq. (7) describes transitions and decoherence within the $|1\rangle$, $|2\rangle$ subspace, and has a simple form in the basis of energy eigenstates of the two-state Hamiltonian (2):

$$\gamma[\rho] = -U^{\dagger}\begin{pmatrix} \gamma_u r_{11} - \gamma_d r_{22}, & \left(\gamma + \dfrac{\gamma_d+\gamma_u}{2}\right) r_{12} \\ \left(\gamma + \dfrac{\gamma_d+\gamma_u}{2}\right) r_{21}, & \gamma_d r_{22} - \gamma_u r_{11} \end{pmatrix} U. \tag{9}$$

Here r is the density matrix in the eigenstate basis: $r = U\rho U^{\dagger}$, and U is the rotation matrix from this basis to the flux basis $|1\rangle$, $|2\rangle$:

$$U = [(1-\varepsilon/\Omega)^{1/2}\sigma_z + (1+\varepsilon/\Omega)^{1/2}\sigma_x]/\sqrt{2},$$

where the σ's denote Pauli matrices, and $\Omega \equiv (\varepsilon^2+\Delta^2)^{1/2}$. The transition rates $\gamma_{d,u}$ and the decoherence rate γ are

$$\gamma_d = \frac{g\Delta^2}{\Omega}\frac{1}{1-e^{-\Omega/T}}, \quad \gamma_u = \gamma_d e^{-\Omega/T}, \quad \gamma = 2gT\frac{\varepsilon^2}{\Omega^2},$$

with the dimensionless parameter $g = 2G(\delta\Phi)^2/\hbar$ characterizing the strength of the interwell relaxation, and we assumed that $G(\omega)$ is constant in the small-frequency range $\omega \sim \Omega$.

Equation (7), with the dissipation terms (8) and (9), is used below to describe resonant tunneling of flux between the two wells in various regimes. Before doing this, we discuss the relative magnitude of the two dissipation terms in this equation. Since the width of the wells is of the same order of magnitude as the barrier between them, the magnitude of the flux matrix elements of the intrawell relaxation $\Gamma[\rho]$, and of the interwell relaxation $\gamma[\rho]$ (determined, respectively, by the ''width'' of the wave functions inside the wells and the distance between the wells) should be close. The main difference between the two relaxation mechanisms is that the intrawell transitions dissipate energy ω_j, whereas the interwell relaxation $\gamma[\rho]$ involves only much smaller energies on the order of ε, Δ, T. This means that the intrawell relaxation typically dominates the flux-tunneling dynamics. In particular, even under the assumed condition of weak relaxation (which for $\Gamma[\rho]$ means that the rates Γ_j are small compared to the oscillation frequencies ω_j) the rates Γ_j can still be much larger than the frequencies ε, Δ of the two-state dynamics. The interwell relaxation $\gamma[\rho]$ will generally only be stronger than the intrawell relaxation if the environment has relatively low cutoff frequency $\omega_c \ll \omega_p$.

III. STATIONARY BIAS

In this section, we calculate the rate of the resonant tunneling between the wells in the situation when the external flux through the SQUID loop does not contain an ac component, and the energy dissipation drives the initial flux state in the left well towards equilibrium. At low temperatures $T \ll \omega_p$ the flux stays initially in the ground state of the left well and then tunnels into the right well out of this state (Fig. 1). In this case, the relaxation rate Γ_1 obviously vanishes. We begin by considering the situation with only the intrawell relaxation present. Equation (7) can then be written in matrix elements as

$$\dot{\rho}_{11} = \Delta \mathrm{Im}\rho_{12}, \quad \dot{\rho}_{22} = -\Delta \mathrm{Im}\rho_{12} - 2\Gamma\rho_{22},$$

$$\dot{\rho}_{12} = -(i\varepsilon+\Gamma)\rho_{12} + (i\Delta/2)(\rho_{22}-\rho_{11}), \tag{10}$$

with $\Gamma_2/2 \equiv \Gamma$ in this section.

After transformation to the real and imaginary parts of the off-diagonal matrix element ρ_{12} and the sum/difference $\rho_{11} \pm \rho_{22}$ of the diagonal elements of the density matrix, Eqs. (10) can be solved directly with the initial condition that the flux is in the left well at time $t=0$, $\rho_{11}(0)=1$:

$$\rho_{11}(t) = \frac{1}{2}\frac{e^{-\Gamma t}}{\omega^2+\lambda^2}\left\{(\Gamma^2+\omega^2)\left[\left(1+\frac{\lambda^2}{\Gamma^2}\right)\times\cosh\lambda t + 2\frac{\lambda}{\Gamma}\sinh\lambda t\right] + (\lambda^2-\Gamma^2)\times\left[\left(1-\frac{\omega^2}{\Gamma^2}\right)\cos\omega t - 2\frac{\omega}{\Gamma}\sin\omega t\right]\right\},$$

$$\rho_{22}(t) = \frac{1}{2}\frac{e^{-\Gamma t}}{\omega^2+\lambda^2}\left[(\Gamma^2+\omega^2)\left(1-\frac{\lambda^2}{\Gamma^2}\right)\times\cosh\lambda t + (\lambda^2-\Gamma^2)\left(1+\frac{\omega^2}{\Gamma^2}\right)\cos\omega t\right]. \tag{11}$$

In Eq. (11), the eigenfrequencies ω and λ of the system of Eqs. (10) are

$$\omega, \lambda = \left[\left(\frac{(\Omega^2-\Gamma^2)^2}{4}+\Gamma^2\varepsilon^2\right)^{1/2} \pm \frac{\Omega^2-\Gamma^2}{2}\right]^{1/2}. \tag{12}$$

Equations (11) contain all the information about dynamics of the flux tunneling. When the relaxation rate Γ_2 is much smaller than the oscillation frequency Ω, the tunneling process consists of the weakly damped coherent oscillations of the flux between the wells followed by relaxation in the right well. With increasing relaxation rate the oscillation part of this process becomes increasingly more damped and turns into incoherent jumps of the flux from the left into the right well represented by the non-oscillatory exponential decay of ρ_{11}.

The matrix element $\rho_{11}(t)$ has the meaning of the probability for the flux to remain in the left well at time t. In the case of monotonous decay of ρ_{11}, its derivative $f(t)=-[\rho_{11}(t)]'$ gives the probability density of the time for flux tunneling between the wells. This probability density can be used to find all statistical characteristics of the flux tunneling process. For instance, the average time τ it takes for the flux to tunnel can be calculated as $\tau=\int_0^\infty dt\ tf(t)=\int_0^\infty dt\rho_{11}(t)$. In the coherent regime, when $\rho_{11}(t)$ oscillates in time, $f(t)$ can be negative and cannot be interpreted as probability density, and the question of how to define the tunneling time τ becomes nontrivial. To define τ, one needs to establish the event that terminates the tunneling process. The definition adopted below assumes that the tunneling process ends when the flux makes the transition from the state $|2\rangle$ into one of the lower energy states in the right well. This definition is motivated by the fact that such a transition eliminates the possibility for the flux to return into the left well. With such definition, the time the flux spends in the state $|2\rangle$ is included in the tunneling time τ which then should be calculated as

$$\tau=\int_0^\infty dt[\rho_{11}(t)+\rho_{22}(t)]. \tag{13}$$

From Eqs. (11) and (13) we obtain the tunneling rate

$$\tau^{-1}=\frac{\Delta^2\Gamma_2}{2\Delta^2+\Gamma_2^2+4\varepsilon^2}. \tag{14}$$

Equation (14) describes the Lorentzian peak of the resonant flux tunneling. It shows that the resonant flux tunneling under stationary-bias conditions does not allow one to distinguish qualitatively between the regimes of coherent and incoherent flux tunneling since the shape of the resonance peak (14) remains the same regardless of the magnitude of the relaxation/decoherence rate Γ.

The average tunneling rate τ^{-1} can be calculated without explicit solution of the time-dependent equations for the density matrix. Instead of attempting to describe an individual tunneling event with the time-dependent solution, we can consider a large number of these events, assuming that after each transition from the left to the right well the system is immediately returned back to its initial state and the process is repeated. This immediate return means that the system is effectively decaying from the resonant state in the right well directly into the initial state in the left well, and can be modeled by adding the term $\Gamma_2\rho_{22}$ into the equation for ρ_{11}. With such a modification, Eq. (7) has a nontrivial stationary solution $\rho^{(0)}$, and the tunneling rate τ^{-1} defined by Eq. (13) can be found from this solution as

$$\tau^{-1}=\Gamma_2\rho_{22}^{(0)}. \tag{15}$$

Since this method does not require solution of the time-dependent equations for the density matrix, it considerably simplifies the calculation of the average tunneling rate.

To illustrate this procedure, we consider first the same tunneling under the stationary bias conditions described by Eqs. (10) with the term $\Gamma_2\rho_{22}$ included into the equation for ρ_{11}. Solving the stationary equation for the off-diagonal element ρ_{12} of the density matrix and plugging the solution into the equations for the diagonal elements, we get the simple rate equations

$$\dot\rho_{11}=\Gamma'(\rho_{22}-\rho_{11})+\Gamma_2\rho_{22},\quad \dot\rho_{22}=-\dot\rho_{11}, \tag{16}$$

where the transfer rate $\Gamma'=\Delta^2\Gamma_2/(\Gamma_2^2+4\varepsilon^2)$ between the two wells can be viewed as the ''golden-rule'' rate of transition with the matrix element $\Delta/2$ into the state $|2\rangle$ broadened by the relaxation Γ_2. From the stationary solution of Eq. (16) we find that $\rho_{22}^{(0)}=\Gamma'/(\Gamma_2+2\Gamma')$, and see that Eq. (15) indeed reproduces the tunneling rate (14).

The tails of the resonant peak (14) at $\varepsilon\gg\Delta,\Gamma_2$ allow for another simple interpretation. At large ε, the wave function of the eigenstate of the two-state Hamiltonian localized in the left well has the probability amplitude $\Delta/2\varepsilon$ in the right well. The tunneling rate $\overline{\Gamma}$ in this regime can be found then as the probability to be in the right well times the relaxation rate Γ_2:

$$\overline{\Gamma}=\Gamma_2\Delta^2/4\varepsilon^2. \tag{17}$$

This simple reasoning indeed reproduces the tails of the peak (14) and allows us to obtain an estimate of the tunneling rate between the resonances. As shown in the Appendix, the wave function amplitude in the right well between the resonances is $\pi\Delta/[2\omega_2\sin(\pi\varepsilon/\omega_2)]$. From this we can write

$$\tau^{-1}=\Gamma_2\left(\frac{\pi\Delta}{2\omega_2\sin(\pi\varepsilon/\omega_2)}\right)^2. \tag{18}$$

It should be noted that Eq. (18) is only an estimate, since Γ_2 and Δ depend on ε for $\varepsilon\sim\omega_2$, and can be different from their values at resonance. However, at $\varepsilon\ll\omega_2$, they are constant, and Eqs. (14) and (18) coincide for $\varepsilon\gg\Delta,\Gamma_2$. In this range of ε the tunneling rate τ^{-1} changes as ε^{-2}.

If the interwell relaxation is non-negligible, we need to keep both relaxation terms in Eq. (7). The assumption that the relaxation rates are small in comparison with Δ, allows us to use Eq. (9) for the interwell relaxation and makes it convenient to consider the flux dynamics in the eigenstates basis. The stationary values of the off-diagonal elements of the density matrix r in this basis are vanishing for weak relaxation. To find the diagonal elements of r, we transform Eq. (8) for the intrawell relaxation (with $\Gamma_1=0$ and added term $\Gamma_2\rho_{22}$ in the evolution of ρ_{11}) into this basis. Neglecting rapidly oscillating terms, we see that the diagonal part of the weak intrawell relaxation is

$$\dot r_{11}=\Gamma_2\left[\frac{-\varepsilon}{2\Omega}+\frac{1}{4}\left(1+\frac{\varepsilon^2}{\Omega^2}\right)(r_{22}-r_{11})\right],\quad \dot r_{22}=-\dot r_{11}.$$

Combining this expression with Eq. (9) for the interwell relaxation, we find the stationary values of the diagonal elements of r. After transformation back to the flux basis we finally obtain the stationary element $\rho_{22}^{(0)}$ of the density matrix ρ in the flux basis and the flux tunneling rate (15):

$$\tau^{-1}=\frac{\Gamma_2}{2}\,\frac{\Omega\coth(\Omega/2T)+\varepsilon+\mu}{\Omega\coth(\Omega/2T)+\mu(1+2\varepsilon^2/\Delta^2)}, \tag{19}$$

$$\mu\equiv\Gamma_2/2g.$$

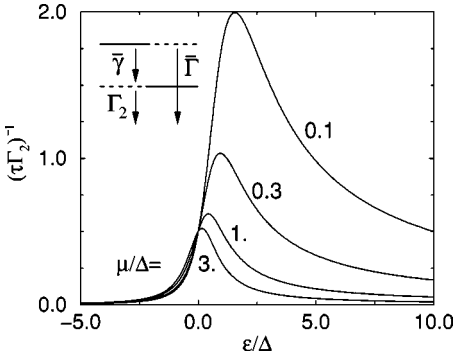

FIG. 2. The zero-temperature rate τ^{-1} of flux tunneling between the wells of the double-well potential as a function of the energy bias ε for different values of μ, which characterizes the relative strength of the two relaxation mechanisms (19). The inset shows the diagram of the off-resonant transitions.

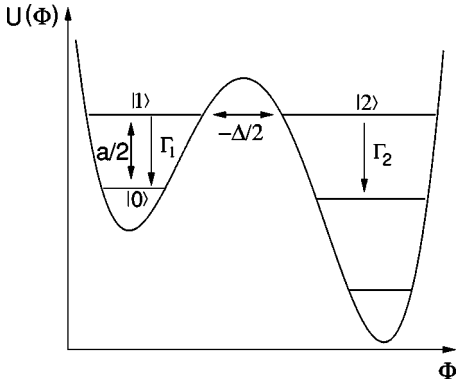

FIG. 3. Schematic diagram of the ''photon-assisted'' macroscopic resonant tunneling of flux stimulated by an rf perturbation of strength $a/2$.

The parameter μ in Eq. (19) can be interpreted as the energy at which the characteristic interwell relaxation rate (which increases with the energy difference between the two resonant states) becomes equal to the rate Γ_2 of the relaxation in the right well. The tunneling rate (19) is plotted in Fig. 2 for zero temperature and several values of μ. The interwell relaxation becomes stronger with decreasing μ, making the the resonant-tunneling peak progressively more asymmetric. For negative bias ε, when the state $|2\rangle$ in the right well is higher in energy than the state $|1\rangle$ in the left well, the interwell relaxation is suppressed for low temperatures, $T \ll \Delta$, and the tail of the resonant peak (19) coincides with that of the Lorentzian peak (14). On the other ha nd, for positive ε, transitions from the state $|1\rangle$ into $|2\rangle$ are allowed, and if $\mu \leqslant \Delta$, the interwell relaxation dominates for all positive ε. The tunneling rate decreases in this case only as $1/\varepsilon$ with increasing ε.

At $\varepsilon \gg \Delta$, and vanishing temperature T, the tunneling rate (19) determined by the interplay between the interwell and intrawell relaxation can be understood in terms of the competition between the two tunneling paths (see inset in Fig. 2). One is the direct decay within the right well out of the eigenstate of the two-state Hamiltonian localized predominantly in the left well, but with a small probability amplitude in the right well. The rate of this decay is $\bar{\Gamma}$ (17). Another is the transition between the two eigenstates induced by the interwell relaxation that transfers the probability between the two wells and is followed by the intrawell decay out of the lower-energy eigenstate with the rate Γ_2. The rate of the interwell transition between the eigenstates is

$$\bar{\gamma} = \frac{g\Delta^2}{\varepsilon}. \tag{20}$$

At $\mu < \Delta$, the second path dominates, and for sufficiently large ε, $\varepsilon \gg \Delta^2/\mu$, the bottleneck of the relaxation process is the interwell transition between the eigenstates and the tunneling rate (19) becomes independent of the intrawell rate Γ_2: $\tau^{-1} = \bar{\gamma}$. In general, the competition between the two types of transitions gives an expression for the tunneling rate, $\tau^{-1} = \Gamma_2(\bar{\gamma}+\bar{\Gamma})/(\bar{\gamma}+\Gamma_2)$, that agrees with Eq. (19) at $\varepsilon \gg \Delta$.

For large μ, $\mu \gg \Delta$, the interwell relaxation is weak close to resonance, and for sufficiently small bias, $\varepsilon \ll \mu$, Eq. (19) coincides with Eq. (14) with $\Gamma_2 \ll \Delta$. However, at larger bias, $\varepsilon \gg \mu$, the interwell relaxation increases and the tunneling rate is again given by $\bar{\gamma}$ (20). Only when μ becomes comparable to the level separation ω_p in the wells, the interwell relaxation is completely negligible and the resonant tunneling peak has the Lorentzian shape for all relevant energies.

Away from resonance, when $\varepsilon \sim \omega_p$, the interwell tunneling with the rate (20) corresponds to the transitions between the states localized in opposite wells that are the closest in energy, while ''intrawell'' tunneling (18) corresponds to the transition between the states that are at least next-nearest neighbors in energy. Although there is no qualitative difference between the two types of the transitions away from the resonance, they lead to very different shapes for the tunneling peaks close to resonance.

IV. PHOTON-ASSISTED TUNNELING

When the SQUID is irradiated with an external rf signal, the macroscopic resonant flux tunneling can go more effectively through one of the excited states in the left well of the SQUID potential rather than out of the ground state, since the amplitude of tunneling $-\Delta/2$ out of the excited state is much larger than the tunneling amplitude for the ground state. In this section, we consider the situation when an rf signal of frequency ω resonantly couples the ground state $|0\rangle$ in the left well of the potential to an excited state $|1\rangle$ with energy E in this well (Fig. 3). The energy E is on the order of ω_p, and the condition of the resonant excitation is that the detuning $\nu = E - \omega$ is small, $\nu \ll \omega_p$. If the amplitude a of the rf excitation is also relatively small, $a \ll \omega_p$, the off-resonant coupling to other states[27] is not important, and the coupling between the states $|0\rangle$ and $|1\rangle$ can be described in the rotating-wave approximation. In this approximation, the terms in the coupling that oscillate rapidly (with frequencies on the order of ω_p) are neglected, and the coupling Hamiltonian is written as

$$H_{rf} = \frac{a}{2}(|0\rangle\langle 1|e^{-i\nu t} + |1\rangle\langle 0|e^{+i\nu t}). \tag{21}$$

If the excited state $|1\rangle$ in the left well is coupled resonantly with amplitude $-\Delta/2$ to a state $|2\rangle$ in the right well that is shifted in energy by ε with respect to $|1\rangle$, the total Hamiltonian for the flux dynamics in the basis of the three states $|0\rangle$, $|1\rangle$, and $|2\rangle$ is

$$H_0=\begin{pmatrix} 0 & a/2 & 0 \\ a/2 & \nu & -\Delta/2 \\ 0 & -\Delta/2 & \nu-\varepsilon \end{pmatrix}. \tag{22}$$

As in the previous section, the average flux tunneling rate τ^{-1} can be calculated according to Eq. (15) from the stationary density matrix ρ of the system in the basis of states $|0\rangle$, $|1\rangle$, and $|2\rangle$. Time evolution of ρ is described by the same Eq. (7) but with the Hamiltonian H_0 given now by Eq. (22). We begin discussion of the dynamics of flux tunneling in the three-state system (22) with the case when the interwell relaxation $\gamma[\rho]$ can be neglected, and the only mechanism of the energy relaxation in the system is the intrawell relaxation $\Gamma[\rho]$. This relaxation is characterized by the two rates $\Gamma_{1,2}$ of the transitions from the states $|1,2\rangle$ into the lower energy states of the left and right potential well, respectively (Fig. 3). An obvious generalization of Eq. (8) for $\Gamma[\rho]$ to the three-state basis gives the off-diagonal part of Eq. (7) for the time evolution of ρ of the following form:

$$\begin{aligned}
\dot{\rho}_{01}&=(i\nu-\Gamma_1/2)\rho_{01}+ia(\rho_{00}-\rho_{11})/2-i\Delta\rho_{02}/2,\\
\dot{\rho}_{12}&=-(i\varepsilon+(\Gamma_1+\Gamma_2)/2)\rho_{12}+i\Delta(\rho_{22}-\rho_{11})/2-ia\rho_{02}/2,\\
\dot{\rho}_{02}&=(i(\nu-\varepsilon)-\Gamma_2/2)\rho_{02}-ia\rho_{12}/2-i\Delta\rho_{01}/2.
\end{aligned} \tag{23}$$

Equations (23) allow us to express the off-diagonal elements of ρ in terms of the diagonal ones in the stationary regime. Inserting the stationary values of the off-diagonal elements into the equations for the diagonal elements

$$\begin{aligned}
\dot{\rho}_{00}&=-a\,\mathrm{Im}\,\rho_{01}+\Gamma_1\rho_{11}+\Gamma_2\rho_{22},\\
\dot{\rho}_{11}&=a\,\mathrm{Im}\,\rho_{01}+\Delta\,\mathrm{Im}\,\rho_{12}-\Gamma_1\rho_{11},\\
\dot{\rho}_{22}&=-\Delta\,\mathrm{Im}\,\rho_{12}-\Gamma_2\rho_{22},
\end{aligned} \tag{24}$$

we calculate the stationary probability $\rho_{22}^{(0)}$ and find the flux tunneling rate (15).

Equations (24) were written under the assumption that the relaxation in the left well b rings the system out of the state $|1\rangle$ directly into the ground state $|0\rangle$. Although this is strictly true only in the case when $|1\rangle$ is the first excited state in the well, Eqs. (24) can be also used to calculate the average flux tunneling rate in other situations. Indeed, when the rf signal drives the system into the state $|1\rangle$ that is not the first excited state, the intermediate states in the left well that exist between the states $|0\rangle$ and $|1\rangle$ are populated by the process of relaxation out of $|1\rangle$. If the flux tunneling out of these states is neglected (similarly to tunneling out of the state $|0\rangle$), their effect on the average tunneling rate can be accounted for by inclusion of the occupation probabilities of these states in the normalization condition. Since these probabilities in the stationary regime are proportional to the stationary occupation probability ρ_{11}, this can be done through an additional factor λ in the normalization condition for the state $|0\rangle$, $|1\rangle$, and $|2\rangle$:

$$\rho_{00}+\lambda\rho_{11}+\rho_{22}=1. \tag{25}$$

To give an example, we can calculate the factor λ assuming that the left well is parabolic in the relevant energy range. Then, the standard result for the linear relaxation of the harmonic oscillator (see, e.g., Ref. 28) is that the oscillator makes the transitions only between the nearest-neighbor states and that the transition rate from the state $|m\rangle$ into $|m-1\rangle$ is proportional to m. This means that in the stationary state $\rho_{m-1,m-1}=m\rho_{m,m}/(m-1)$, and if the rf radiation drives the system into the nth excited state of the left well, then $\lambda=n\Sigma_{m=1}^{n}(1/m)$. To avoid extra parameters, however, we assume from now on that the state $|1\rangle$ is the first excited state in the left well, so that $\lambda=1$.

Sufficiently compact analytical expressions for the tunneling rate can be obtained from Eqs. (23) and (24) only in certain limits. For example, for small rf amplitude and weak relaxation, $a\ll\Gamma_{1,2}\ll\Delta$, we get[29]

$$\tau^{-1}=\frac{\Gamma_2 a^2\Delta^2}{(2\nu-\varepsilon-\Omega)^2(2\nu-\varepsilon+\Omega)^2+4[\Gamma_1(\nu-\varepsilon)+\Gamma_2\nu]^2}. \tag{26}$$

Equation (26) describes two peaks (discussed in more details below) in the dependence of the tunneling rate on the detuning ν. The peaks are broadened by the relaxation, and their positions correspond to the two eigenstates of the Hamiltonian (2): $\nu=(\varepsilon\pm\Omega)/2$. Another expression for the tunneling rate can be obtained for large relaxation rates $\Gamma_{1,2}\gg a,\Delta$:

$$\tau^{-1}=\frac{\Gamma_2 a^2\Delta^2}{(4\nu^2+\Gamma_1^2)[4(\nu-\varepsilon)^2+\Gamma_2^2]}. \tag{27}$$

Depending on the relation between the energy bias ε and the relaxation rates, the tunneling rate (27) as a function of detuning ν contains either one (for small ε) or two separate peaks (for large ε). The peak positions in this case coincide with the position of the energy levels $|1,2\rangle$ localized in the two wells.

For arbitrary parameters it is convenient to use the stationary solution of Eqs. (23) and (24) to plot the tunneling rate τ^{-1} numerically. To simplify the discussion, we assume that the relaxation rates in the two wells are the same, $\Gamma_1=\Gamma_2\equiv\Gamma$. Figure 4 shows the dependence of τ^{-1} on detuning ν obtained in this way for several rf amplitudes a in the regime of small relaxation rate Γ. The main qualitative feature of Fig. 4 [that can also be seen in Eq. (26)] is that for small a the resonant peak in the tunneling rate τ is split into two peaks due to coherent oscillations of flux between the two wells. The appearance of such splitting can be easily understood, since a weak rf signal excites the system not into the state $|1\rangle$ localized in the left well, but into the two hybridized states formed out of the states $|1\rangle$ and $|2\rangle$ in the two wells. The two different energies of the two hybridized states lead to the two peaks in the tunneling rate. This means that the splitting of the resonant-tunneling peak is the direct

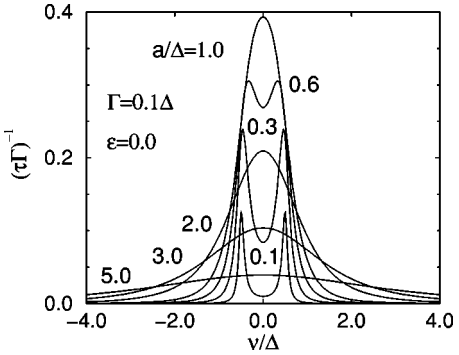

FIG. 4. The rate τ^{-1} of the photon-assisted resonant tunneling of flux Φ between the two wells of the SQUID potential as a function of detuning ν for several values of the rf amplitude a. For discussion see the text.

manifestation of the quantum coherent oscillations of flux between the two wells of the SQUID potential.

Figure 4 illustrates also how the splitting of the resonant tunneling peak is suppressed with the increase of the rf amplitude. Suppression of the peak splitting can be understood in terms of the time $1/\Delta$ required to establish the stationary states hybridized between the two wells. Large rf amplitude a on the order of the tunnel amplitude Δ causes rapid Rabi oscillation between the states $|0\rangle$ and $|1\rangle$ and does not allow for sufficient time to establish the two hybridized states. The system is therefore effectively excited into the state $|1\rangle$ localized in the left well, and single resonant tunneling peak is formed around the energy of this state. Broadening and suppression of this single peak seen in Fig. 4 as a increases beyond Δ, is a version of the generic ''quantum Zeno'' effect, when tunneling out of a metastable state is suppressed by rapid perturbation of this state.

Figure 5 shows the evolution of the coherently split tunneling peaks at small rf amplitude a with the bias energy ε and with the relaxation rate Γ. We see that with increasing energy bias [Fig. 5(a)], the peaks follow the position of the energy levels and the splitting between them increases. Simultaneously, the peak height decreases reflecting the overall suppression of the tunneling rate as one moves away from the resonance. Figure 5(b) shows how the double-peak structure in the small-bias regime representing the coherent mixing of the flux states in the two wells is suppressed by increasing relaxation rate Γ. The structure is visible up to the relaxation rates $\Gamma \simeq 0.5\Delta$.

The peaks in Fig. 5 are shown only for $\varepsilon \geqslant 0$. The peak structure for negative ε can be understood from the ''symmetry'' relation $\tau^{-1}(-\nu,-\varepsilon)=\tau^{-1}(\nu,\varepsilon)$ that can be deduced from Eqs. (23) and (24). Equations (23) show that in the stationary regime, changing the sign of ν,ε is equivalent to changing the sign of a,Δ and replacing the off-diagonal elements of ρ with their complex conjugate values. This transformation obviously does not change the transition rates in Eq. (24), and therefore does not change the flux tunneling rate τ^{-1}.

Another interesting manifestation of the coherent flux tunneling between the wells can be seen in the dependence of the tunneling rate on the bias energy ε at fixed detuning ν (Fig. 6). For weak relaxation, the hybridized states are well developed, and when the rf excitation energy lies between

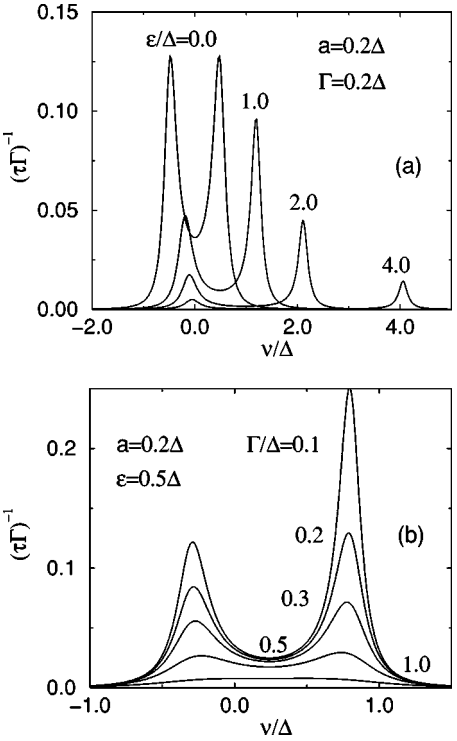

FIG. 5. Evolution of the double-peak structure in the rate τ^{-1} of the photon-assisted resonant flux tunneling as a function of detuning ν with increasing (a) bias energy ε and (b) relaxation rate Γ.

these two states, the tunneling rate is strongly suppressed. At $\nu=0$, when the system is excited precisely into the state $|1\rangle$ localized in the left well, this condition is satisfied and tunneling rate is strongly suppressed for any energy bias ε. As can be seen from Eq. (26) and Fig. 6, in this case the tunneling rate as a function of ε is described by a Lorentzian centered around $\varepsilon=0$. In contrast to resonant tunneling peaks in the ν dependence of the tunneling rate, which have small width proportional to the relaxation rate Γ, the width of this Lorentzian is large Δ^2/Γ, and is inversely proportional to Γ. When the detuning ν deviates from zero, there is an energy bias ε at which the excitation energy coincides with the energy of one of the hybridized states. The tunneling rate has a peak under such resonance conditions. For not-too-small ν's, this resonant peak again has a small width proportional to Γ.

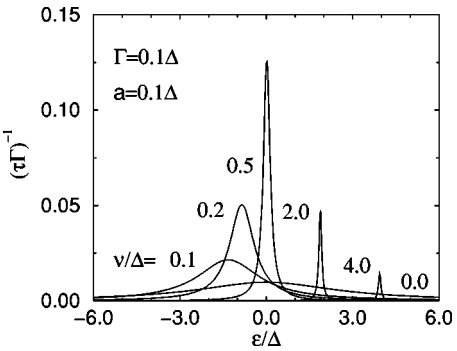

FIG. 6. Bias-energy dependence of the photon-assisted flux tunneling rate at fixed detuning ν for small rf amplitude and relaxation rate Γ. For vanishing detuning, the tunneling rate exhibits a very broad maximum with a width inversely proportional to Γ.

In Fig. 6, one can see how the transition between the broad and narrow tunneling peaks takes place for $\nu \geqslant 0$. As before, the results for negative detuning can be deduced from the relation $\tau^{-1}(-\nu,-\varepsilon)=\tau^{-1}(\nu,\varepsilon)$.

It should be noted also that the fact that each curve in Fig. 6 has only one peak of the tunneling rate τ^{-1} does not contradict the experimental results[22] which show double peak structure in the dependence of τ^{-1} on the external flux Φ_e through the SQUID loop, which controls the bias energy ε. The reason for this is that for experimental SQUID parameterers, variations of Φ_e change not only ε but the energy separation of the states within the same well also, and therefore affect the detuning ν.

Finally, we discuss the effect of weak interwell relaxation on the photon-assisted tunneling. We start by generalizing Eq. (9) for this relaxation to the three-state situation relevant for the photon-assisted tunneling. Under the natural assumption that the average flux in the states $|0\rangle$ and $|1\rangle$ in the left well of the SQUID potential is the same, the part of the dissipative coupling (3) that corresponds to the interwell relaxation is

$$V=-I_f\delta\Phi\begin{pmatrix}1&0&0\\0&1&0\\0&0&-1\end{pmatrix}\equiv -I_f\delta\Phi U. \tag{28}$$

While Eq. (28) is written in the flux basis $|0\rangle,|1\rangle,|2\rangle$, weak relaxation is conveniently described in the basis of the eigenstates $|n\rangle$ of the Hamiltonian (22). In this basis, the contribution of the interwell relaxation (28) to the evolution of the density matrix ρ is given by the standard expression similar to Eq. (9):

$$\dot{\rho}_{nn}=\sum_m\ (\gamma_{mn}\rho_{mm}-\gamma_{nm}\rho_{nn}), \tag{29}$$

$$\dot{\rho}_{nm}=-\left[\gamma'_{mn}+\frac{1}{2}\sum_k\ (\gamma_{nk}+\gamma_{mk})\right]\rho_{nm},\quad n\neq m.$$

Transition and dephasing rates in these equations are

$$\gamma_{nm}=\frac{g|U_{nm}|^2(\varepsilon_n-\varepsilon_m)}{1-e^{-(\varepsilon_n-\varepsilon_m)/T}},\quad \gamma'_{nm}=\frac{gT}{2}(U_{nn}-U_{mm})^2,$$

where U_{nm} are the matrix elements of the operator U (28) in the eigenstates basis, and ε_n is the energy of the eigenstate $|n\rangle$.

Interwell relaxation can be included into the evolution equations for the density matrix on the basis of Eq. (29) numerically. We diagonalize the Hamiltonian (22), calculate the interwell relaxation terms (29) in the eigenstates basis, and transfer them into the flux basis, where the intrawell relaxation has the simple form (23), (24). Calculating finally the stationary value of the density matrix ρ we find the flux tunneling rate (15).

Figures 7 and 8 show results of such a calculation obtained at vanishing temperature T. In Fig. 7, the tunneling rate is plotted as a function of the detuning ν for $\varepsilon=0$ and several values of the relative strength of the intrawell relaxation Γ. The eigenstates of the two-state Hamiltonian at $\varepsilon=0$ are symmetric between the two wells, and in absence of the interwell relaxation produce two symmetric resonant tunneling peaks [see Figs. 4 and 5(a)]. As can be seen from Fig. 7, the interwell relaxation makes the tunneling peaks asymmetric. The positive-ν side of the double-peak structure corresponds to excitation of the system into the lower-energy eigenstate and is unaffected by the interwell relaxation at zero temperature, since there is no energy in this regime to create additional tunneling path. In contrast, the negative-ν side of the double-peak structure corresponds to excitation of the system into the eigenstate with larger energy, and the

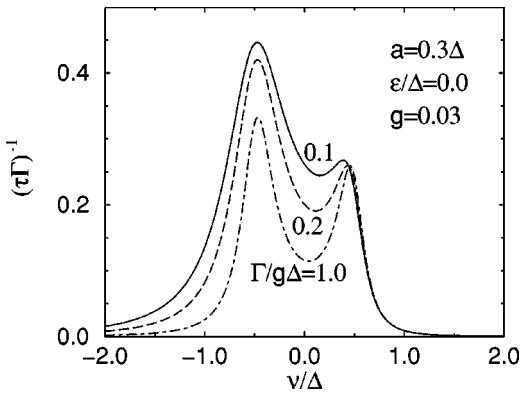

FIG. 7. The rate τ^{-1} of the photon-assisted flux tunneling as a function of the detuning ν in the case of symmetric coupling between the tunneling flux states, $\varepsilon=0$, in the presence of both interwell and intrawell relaxation. Different curves correspond to different magnitudes of the intrawell relaxation rate Γ relative to the interwell relaxation rate.

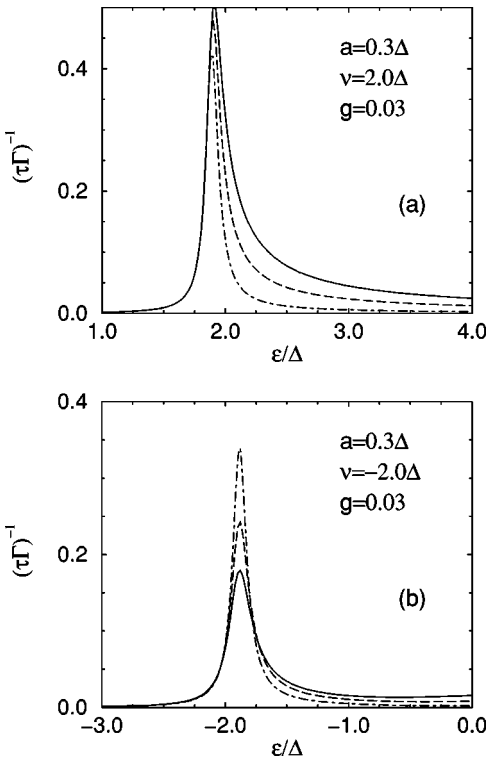

FIG. 8. The rate τ^{-1} of the photon-assisted flux tunneling as a function of the bias energy ε for two ''symmetric'' values of the detuning ν and the same rates of the intrawell relaxation Γ as in Fig. 7. In (a), τ^{-1} decreases with increasing Γ for ε above the peak, while in (b), the peak height increases with Γ.

interwell relaxation increases the rate of tunneling out of this state. Because of this, the negative-ν peak in Fig. 7 is larger than the tunneling peak at positive ν, and the tunneling rate at $\nu<0$ decreases much more slowly away from the peak than at positive ν.

Interwell relaxation introduces asymmetry also in the dependence of the flux tunneling rate on the bias energy ε. Examples of such dependence are shown in Fig. 8 for two values of the detuning, $\nu=\pm 2\Delta$. In both cases, the tunneling rate has a resonant peak at $\varepsilon\simeq\nu$ similar to the peaks shown in Fig. 6 for vanishing interwell relaxation, when the peaks for the two values of detuning are symmetric. Comparison of Figs. 8(a) and 8(b) shows that the interwell relaxation makes the peaks asymmetric. In particular, the peak at $\nu<0$ is smaller than the peak at $\nu>0$. Although this asymmetry appears to be opposite to that in Fig. 7, where the negative-ν peak is larger, it has the same origin as in Fig. 7. The peaks at $\nu<0$ and $\nu>0$ correspond to resonant excitation of the system into, respectively, the upper and lower energy eigenstates. When the resonance occurs for $|\varepsilon|>\Delta$, as in Fig. 8, the eigenstates are already to a large extent localized in one or the other well. At $\varepsilon\simeq\nu>0$, the lower eigenstate is centered in the right well and the interwell relaxation increases the tunneling rate, while at $\varepsilon\simeq\nu<0$ the lower eigenstate is centered in the left well and the interwell relaxation brings the system back to this well suppressing the tunneling rate. As a result, the resonant tunneling peak in Fig. 8(a) ($\nu>0$) is larger than in Fig. 8(b) ($\nu<0$). The height of the negative-ν peak is more sensitive to the relative strength of the two relaxation mechanisms and decreases with decreasing rate Γ of the intrawell relaxation.

The tails of the photon-assisted resonant peaks can be described analytically. When the bias energy and detuning are not close to any resonance, $|\nu|,|\varepsilon|,|\nu-\varepsilon|\gg a,\Delta$ both the interwell tunneling and rf excitation can be treated as perturbations. The dynamics of flux tunneling in this regime can be described as a coexistence of the two tunneling paths similar to the off-resonant tunneling discussed in Sec. II (see inset to Fig. 2). If $\nu>\varepsilon$, the effective energy $\nu-\varepsilon$ of the state $|2\rangle$ in the right well [i.e., the energy of this state brought down by a quantum of rf radiation, as in the Hamiltonian (22)] is above the energy of the initial state $|0\rangle$ in the left well, and the only energy-allowed tunneling path is direct relaxation in the right well out of the perturbed state $|0\rangle$. Similarly to Eq. (17), perturbation theory in a,Δ gives for the rate $\overline{\Gamma}$ of this tunneling:

$$\overline{\Gamma}=\frac{\Gamma_2 a^2\Delta^2}{16\nu^2(\nu-\varepsilon)^2}. \tag{30}$$

If $\nu<\varepsilon$, the effective energy of the state $|2\rangle$ is lower than the energy of the state $|0\rangle$, and in addition to the tunneling (30) there is a competing tunneling process. It consists of a transition between the perturbed states $|0\rangle$ and $|2\rangle$ with the rate $\overline{\gamma}$,

$$\overline{\gamma}=\frac{g a^2\Delta^2}{4\nu^2(\varepsilon-\nu)}, \tag{31}$$

that is driven by interwell relaxation, followed by direct relaxation in the right well with the rate Γ_2. As in Sec. II, the coexistence of the two tunneling paths gives the following total tunneling rate:

$$\tau^{-1}=\Gamma_2\frac{\overline{\gamma}+\overline{\Gamma}}{\overline{\gamma}+\Gamma_2}. \tag{32}$$

One can check that Eqs. (30) and (32) agree, respectively, with the negative-ϵ tail of the resonant tunneling peak in Fig. 8(b) and the positive-ϵ tail of the peak in Fig. 8(a).

In summary, we have studied the effects of two types of relaxation mechanisms on the macroscopic resonant tunneling of flux in SQUID's under stationary-bias conditions and with external rf irradiation. Coherent splitting of the resonant-tunneling peaks by rf radiation provides a convenient way of studying quantum coherence of flux states.

ACKNOWLEDGMENT

This work was supported by ARO Grant No. DAAD199910341.

APPENDIX

In the Appendix we show explicitly how the Hamiltonian of the two-well system (1) can be reduced at resonance to the two-state form (2), and derive an expression for the tunneling amplitude Δ. Assuming that the transparency D of the barrier separating the two wells is small, $D\ll 1$, and that the resonance occurs between the states with large n, we can use the WKB approximation for the wave functions $\psi_{jn}(\Phi)$ of the Hamiltonian (1). In this approximation, the wave function between the right and the left turning points r and l is

$$\psi(\Phi)=\frac{A}{\sqrt{p}}\cos[w(\Phi)-\delta], \tag{A1}$$

with the WKB phase $w(\Phi)=(1/\hbar)\int_l^\Phi d\Phi' p(\Phi')-\pi/4$ and momentum $p=2C[E-U(\Phi)]^{1/2}$. In Eq. (A1), δ is a constant phase shift, and A is a normalization constant. The phase w is defined in such a way that $\delta=0$ for an isolated well, when the wave function decays exponentially in the classically inaccessible region $\Phi>r,\Phi<l$. When the two wells are coupled, the energy E of the state common to them deviates from the eigenenergies ε_n of the isolated wells that are determined by the Bohr-Sommerfeld condition $(1/\hbar)\int_l^r p d\Phi=2\pi(n+1/2)$. For weak tunneling, this deviation is small in comparison to the state energy, and creates a small but nonvanishing phase shift δ:

$$\delta=\frac{1}{\hbar}\int_l^r[p(E)-p(\varepsilon_n)]=\pi\frac{E-\varepsilon_n}{\omega_p}, \tag{A2}$$

where ω_p is the frequency of the classical oscillations in the well which in the WKB approximation determines the spacing of the energy levels.

At nonvanishing δ, the wave function (A1) has a part that grows exponentially in the classically inaccessible region, as one can see rewriting it as

$$\psi = \frac{Ae^{i\delta}}{\sqrt{p}}\cos w(\Phi) - \frac{iA\sin\delta}{\sqrt{p}}e^{iw(\Phi)}. \quad \text{(A3)}$$

According to general rules of the WKB approximation—see, e.g., Ref. 30, the two terms in this expression produce exponentially decaying and growing components of the wave functions with the amplitudes $Ae^{i\delta}/2$ and $-A\sin\delta$, respectively. To find the energy E we need to match the amplitudes of the wave functions of the right and left wells in the barrier region. Under the conditions of resonance, equating the amplitudes and keeping only the terms of the first order in D we get

$$A_1\frac{E-\varepsilon_1}{\omega_1} = -A_2\frac{D}{2\pi}, \quad A_2\frac{E-\varepsilon_2}{\omega_2} = -A_1\frac{D}{2\pi}, \quad \text{(A4)}$$

where ε_j, $j=1,2$ are the energies of the resonant states, and $D=\exp\{-(1/\hbar)\int_{r_1}^{l_2}|p|d\Phi\}$.

The probability to be in the right/left well is directly related to the wave function amplitudes A_j:

$$\int_{l_j}^{r_j} d\Phi|\psi_j|^2 = \frac{B|A_j|^2}{\omega_j}, \quad \text{(A5)}$$

where B is the j-independent part of the normalization constant. Introducing the amplitudes α of this probability, $\alpha_j = A_j/\omega_j^{1/2}$, we bring Eq. (A4) into the form that coincides with the Schrödinger equation of the two-state system:

$$E\alpha_1 = \varepsilon_1\alpha_1 - \frac{\Delta}{2}\alpha_2, \quad E\alpha_2 = \varepsilon_2\alpha_2 - \frac{\Delta}{2}\alpha_1, \quad \text{(A6)}$$

with the tunneling amplitude

$$\Delta = \frac{(\omega_1\omega_2)^{1/2}}{\pi}D.$$

Since the resonant states $|1,2\rangle$ are orthogonal to all other states of the full Hamiltonian (1), this proves that their dynamics can be described by the Hamiltonian (2).

Away from resonance, when $\varepsilon \equiv \varepsilon_1 - \varepsilon_2 \sim \omega_p$, one of the amplitudes α (for the states localized in the left well, α_2) is small, $\alpha_2 \sim D$. Keeping, as before, only the terms of the first order in D, we see from Eq. (A6) that in this case $E_1 = \varepsilon_1$, i.e., $\delta_1 = 0$. Matching the growing wave function in the right well with the decaying wave function in the left well we find that away from the resonance

$$\alpha_2 = \frac{\pi\Delta}{2\omega_2\sin(\pi\varepsilon/\omega_2)}. \quad \text{(A7)}$$

Equation (A7) extrapolates smoothly between the successive resonances.

Making use of the harmonic approximation for the potential $U(\Phi)$, one can show that the results of this appendix [Eqs. (A6) and (A7)] can be extended to the low-lying states with small n which cannot be described with the WKB approximation. Such an extension leads only to minor modifications in the definition of the barrier transparency D in these equations.

[1] *Quantum Tunneling in Condensed Media*, edited by Yu. Kagan and A.J. Leggett (North-Holland, Amsterdam, 1992).

[2] See, e.g., *Proceedings of the International Conference on Macroscopic Quantum Tunneling and Coherence* [J. Superconduct. **12**, 681 (1999)].

[3] A.J. Leggett and A. Garg, Phys. Rev. Lett. **54**, 857 (1985).

[4] L.E. Ballentine, Phys. Rev. Lett. **59**, 1493 (1987).

[5] A. Peres, Phys. Rev. Lett. **61**, 2019 (1988).

[6] D.V. Averin, Solid State Commun. **105**, 659 (1998).

[7] Yu. Makhlin, G. Schön, and A. Shnirman, Nature (London) **398**, 305 (1999).

[8] L.B. Ioffe, V.B. Geshkenbein, M.V. Feigel'man, A.L. Fauchere, and G. Blatter, Nature (London) **398**, 679 (1999).

[9] J.E. Mooij, T.P. Orlando, L. Levitov, Lin Tian, Caspar H. van der Wal, and Seth Lloyd, Science **285**, 1036 (1999).

[10] R. Rouse, S. Han, and J.E. Lukens, Phys. Rev. Lett. **75**, 1614 (1995).

[11] P. Silvestrini, V.G. Palmieri, B. Ruggiero, and M. Russo, Phys. Rev. Lett. **79**, 3046 (1997).

[12] Yu.N. Ovchinnikov and A. Schmidt, Phys. Rev. B **50**, 6332 (1994).

[13] A. Garg, Phys. Rev. B **51**, 15 161 (1995).

[14] P. Silvestrini, B. Ruggiero, and Yu.N. Ovchinnikov, Phys. Rev. B **54**, 1246 (1996).

[15] A.V. Zhuravlev and A.B. Zorin, Fiz. Nizk. Temp. **16**, 184 (1990) [Sov. J. Low Temp. Phys. **16**, 102 (1990).

[16] J.M. Schmidt, A.N. Cleland, and J. Clarke, Phys. Rev. B **43**, 229 (1991).

[17] D.V. Averin and V.Ya. Aleshkin, Pis'ma Zh. Eksp. Teor. Fiz. **50**, 331 (1989) [JETP Lett. **50**, 367 (1989)].

[18] T.A. Fulton, P.L. Gammel, D.J. Bishop, L.N. Dunkleberger, and G.J. Dolan, Phys. Rev. Lett. **63**, 1307 (1989).

[19] T.H. Stoof and Yu.V. Nazarov, Phys. Rev. B **53**, 1050 (1996).

[20] S.A. Gurvitz, Phys. Rev. B **57**, 6602 (1998).

[21] T. Fujisawa, T.H. Oosterkamp, W.G. van der Wiel, B.W. Broer, R. Aguado, S. Tarucha, and L.P. Kouwenhoven, Science **282**, 932 (1998).

[22] J.R. Friedman, V. Patel, W. Chen, S.K. Tolpygo, and J.E. Lukens, Nature (London) **406**, 43 (2000).

[23] J.E. Mooij (private communication).

[24] K.K. Likharev, *Dynamics of Josephson Junctions and Circuits* (Gordon and Breach, New York, 1986).

[25] A.O. Caldeira and A.J. Leggett, Ann. Phys. (N.Y.) **149**, 374 (1983).

[26] K. Blum, *Density Matrix Theory and Applications* (Plenum, New York, 1981).

[27] T. Dittrich, B. Oelschlägel, and P. Hänggi, Europhys. Lett. **22**, 5 (1993).

[28] B.Ya. Zel'dovich, A.M. Perelomov, and V.S. Popov, Zh. Eksp. Teor. Fiz. **55**, 589 (1968) [Sov. Phys. JETP **28**, 308 (1969)].

[29] Note the misprint in this equation in D.V. Averin, J. Low Temp. Phys. **118**, 781 (2000).

[30] L.D. Landau and E.M. Lifshitz, *Quantum Mechanics* (Pergamon Press, Oxford, 1991), Chap. 7.